Design and Implementation of a Data Acquisition and Processing Method for Precisely Calculating the Location Errors of Five-Axis CNC Machine Tools

Jorge Adan Cubas Brizuela[1] (ID) and Syh-Shiuh Yeh[2] (ID)

[1]National Taipei University of Technology, cubas89@gmail.com
[2]National Taipei University of Technology, ssyeh@ntut.edu.tw

Corresponding author: Syh-Shiuh Yeh, ssyeh@ntut.edu.tw

Abstract. The accuracy of five-axis computer numerical control (CNC) machine tools is the most significant factor during cutting processes. However, this accuracy can be easily compromised, primarily due to the location errors of the machine. The correction of these location errors becomes crucial for improving the machine performance and manufacturing accuracy of the products. This study developed a method for the calculation of location errors using a combination of a touch-trigger probe and a calibration sphere. This study was conducted in three stages: data acquisition, data pre-filtering and error calculation, and data filtering from the calculation results. In particular, the filtering approaches in the data processing stage improved the calculation results. The statistical characteristics of the measured data points and all the possible combinations were further considered to reduce the adverse influence of the measurement errors on the calculation results. The cutting tests performed using an AC-type five-axis CNC machine tool indicate a significant decrease in location errors through the application of error compensation to the calculated results. The obtained results are comparable to existing commercialized calculation procedures. The maximum value of absolute errors decreased significantly, and a reduction rate of 80.00% was achieved. Therefore, the cutting tests validate the ability of the developed approaches to reduce the location errors and its usability in actual five-axis CNC machine tool applications.

Keywords: Location error, Calculation process, Five-Axis CNC machine tool, Touch-trigger probe, Calibration sphere.
DOI: https://doi.org/10.14733/cadaps.2023.522-539

1 INTRODUCTION

Computer numerical control (CNC) machines consist of various subsystems, and are normally used in industrial applications because of their ability to achieve a level of detail and accuracy that cannot be achieved by traditional machines. This has made CNC machines a key element in the

mass production of high-quality pieces. Since these machines are aimed towards the mass production of complex pieces, there are several factors affecting the final result during the cutting process: the most common one being mechanical inaccuracies due to geometric errors between the machine axes. These normally small errors commonly emerge from daily use, or by errors during the cutting process. Even though such errors may seem insignificant, in a machine capable of such accuracy, they may affect the results tremendously and greatly compromise the final result. The presence of errors caused by the kinematics of the machine does not only produce failed pieces, but also directly affects the life of the cutting tools and the machine itself.

In five-axis CNC machine tools, geometric and positional deviations can be observed. For instance, it is necessary to consider the squareness and parallelism between a rotary axis and a translational axis as well as the perpendicular distance between the center lines of both the rotary table axis and swivel axis. In a typical CNC machining tool, more than 70% of geometric errors can be attributed to quasistatic errors. These are defined as errors that are related to the geometry of the machining tool and vary slowly with time [24]. The importance of five-axis CNC machine tools has notably increased over the last few years due to the increased flexibility that they offer in comparison to conventional 3-axis machines. This has also motivated many studies focused on improving the accuracy and production quality by the implementation of various approaches.

Currently, there are numerous methods of testing and improving machining accuracy. These include the ball-bar method in order to determine various geometric errors [6,13,25,26,36], identifying errors through machining tests [1,8,16,23], laser sensors [22,30,36,39], R-test [7,9,14,17], and artifact measurement [28,29]. These methods normally require the use of complex machine movements and accuracy measurement devices. Touch-trigger probes have been extensively used for many years for on-machine measurements of the dimensional accuracy of machining tools and parts due to their simplicity and ease of use [4,18,27,31,37,38]. Therefore, geometric errors can be calculated and identified using touch-trigger probes and probing systems. Using a touch-trigger probe and test piece installed on a five-axis CNC machine tool, Ibaraki et al. [11,12] developed an error map illustrating the position-dependent geometric errors using a rotating axis to change its axial position and orientation. Moreover, uncertainty analysis was performed in order to calibrate the location errors, and the results were used to analyze the effects of linear axes motion on the calibration of rotary axes location errors. Ibaraki and Ota [15] developed a method to calibrate the error map of the rotary axes on a five-axis CNC machine tool by using a touch-trigger probe and a test piece. In comparison to conventional calibration methods, this probing method based on machine measurement could be used to automatically and periodically check and update the built error map for on-machine compensation applications. By utilizing a touch-trigger probe and a test piece installed on the five-axis CNC machine tool, Jiang et al. [21] developed a model-based algorithm for decoupling the squareness errors induced by the movement of the linear and rotary axes. They also proposed a probing procedure to identify the location errors of the five-axis CNC machine tool as the distance moved by the linear axes increased, but without using additional equipment. Based on the on-machine measurement using a touch-trigger probe and artifact, Bi et al. [2] developed a calibration method for calculating the geometric errors of the individual rotary axis in a five-axis CNC machine tool by referring to the coordinates of the measured reference points on the artifact. The calculated geometric errors were then utilized to modify the numerical control files so that the five-axis CNC machine tool could apply a geometric error compensation. Due to the measurement and calibration problems induced by using specifically shaped artifacts for the on-machine measurement of the five-axis CNC machine tools, Rahman and Mayer [32] investigated the reproducibility of the probing results by using an uncalibrated indigenous artifact. The proposed calibration method could also estimate the uncertainties of the estimated machine tool error parameters and quantify calibration quality in real applications. By considering the importance of geometric errors on the machining accuracy of the five-axis CNC machine tools, Huang et al. [10] developed an error measurement and identification method for the rotary axes by using a touch-trigger probe and a test piece installed on the five-axis CNC machine tool. This method measured the coordinates of the reference points

on the test piece with different rotating angles and applied the measured results to calculate the geometric errors of the rotary axis without the influence of the geometric inaccuracies and installation error of the applied test piece. Existing approaches have demonstrated the feasibility of using a set of touch-trigger probes and a test piece for the measurement of the geometric errors of five-axis CNC machine tools. Nevertheless, the measurement and calculation results are significantly affected by the operational methods and inherent characteristics of touch-trigger probes [3,19,20,33,34,35]. To mitigate the adverse influence of using touch-trigger probes, it is extremely important to design and implement a data acquisition and processing method for precisely calculating the geometric errors of five-axis CNC machine tools.

The approach adopted in this study is directly aimed at five-axis CNC machine tools and is implemented by using a touch-trigger probe. Depending on the configuration of the machine, touch-trigger probes are typically used to corroborate the workpiece position and obtain the coordinates of simple fixtures by using three reference positions per rotary axis. Using a combination of touch-trigger probe and calibration sphere, the objective of this study was to design and implement an off-line data acquisition and processing method for precisely calculating the location errors particular to five-axis CNC machine tools. In addition, probing paths, which are usually adopted by commercialized measurement software, were utilized to clarify the precise calculation of location errors using the data acquisition and processing method designed in this study. The proposed approach uses a touch-trigger probe to obtain the coordinates of the calibration sphere at different positions for each rotary axis of the machine. The raw data obtained by the probe is then transformed into a system of equations, which can be used to define the exact position of the rotary axis in space. The calculation method of the error variables was developed based on system simplicity, efficiency, and reliability, while aiming towards the highest accuracy allowed by the hardware. The proposed calculation process focuses mainly on data acquisition and calculation, and can be further split into three phases: namely, environment setup (including positioning of calibration sphere and calibration of touch-trigger probe, working environment, and measurements), positioning measurement (including the measurement of different calibration sphere positions), and data calculation (with consideration to the input parameters and raw calculation data). The results of this study are summarized below:

- Successfully created and tested a data measurement and point selection protocol to obtain meaningful data from points to accurately calculate the location errors.
- Created an iterative, reproducible, and reliable calculation method that can be applied to AC-type machine configuration which can also be extended to other types of machine configuration.
- Created a completely different solution, that can be used in various machines, with a performance that is better than conventional and commercialized methods.
- Successfully validated the approaches proposed in this study, through a machine test with location error compensation, performed on a five-axis CNC machine tool equipped with the FANUC 31i-Model B5 controller.
- Through location error compensation, the maximum value of absolute errors on the test workpiece was reduced from 15 μm to 3 μm (80.00% reduction rate) and the RMS value of errors was reduced from 10.9697 μm to 1.7321 μm (84.21% reduction rate).

This paper is structured as follows. Section 2 describes the process hardware, tool calibration, experimental setup, and detailed process flow for the acquisition of data. Sections 3 to 5 detail the data acquisition, calculation processes, and programming stages that were carried out in order to obtain good data to calculate, analyze and validate the test results, and calculate the location errors of a five-axis CNC machine tool. Section 6 covers the validation of the developed methods using the calculated errors and compensation in a real machining test. Section 7 concludes this paper.

2   HARDWARE DESCRIPTION AND CALIBRATION

2.1   Device Description and Usage

The calibration sphere is a crucial part of the experimental process, and its diameter may vary depending on the provider and needs of each machining center. The calibration sphere used in this study had a diameter of 30 mm, which was actually measured as 29.9996 mm. The micrometer is a high accuracy tool used in the calibration procedure as well as in the measurement of environment reference distances, such as table-spindle height and the highest point of the calibration sphere. It is also used to ensure the concentricity of the touch-trigger probe with respect to the machine's spindle axis. The touch-trigger probe was the main tool used during the procedure and was designed to be the data source of the calculation system. The concentricity of the stylus is of tremendous importance in every test since it should maintain a reliable and constant measurement regardless of the touching direction it is being used in. The deformation of the stylus also constitutes an error that should be calculated since the probe should be deformed until it reaches a point that will trigger the inner sensors [5]. As the contact velocity directly affects the tool sensitivity, a feed rate of 10 mm/min was selected after several tests to move the touch-trigger probe and to minimize measurement errors.

This study was conducted using a five-axis AC-type CNC machine tool, which utilized the FANUC controller series 31i-Model B5, as illustrated in Figure 1. A laptop computer with Intel Core i7-4800MQ, 2.7-GHz CPU, and 64-bit Microsoft Windows 8.1 operating system was utilized to implement the system developed in this study. Moreover, MATLAB R2014a software was used for the calculations and simulations in this study.
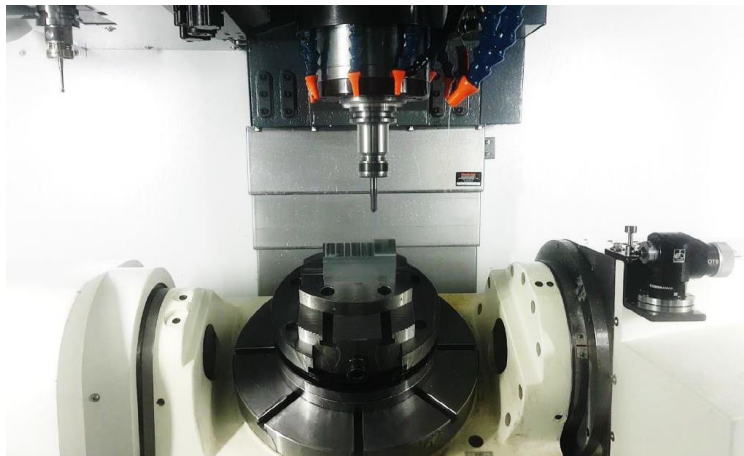

Figure 1: Working space of the five-axis CNC machine tool employed in this study.

2.2   Procedure for Data Acquisition and Calculation

In this study, the following phases were established for data acquisition and calculation:
A. Device calibration phase:
- The machine's rotary plate surface was cleaned and the calibration sphere was fixed with the C-axis at the zero position.
- The length between the rotary table of the machine (C-axis) and the spindle at its zero Z position was measured and recorded for further use.
- The touch-trigger probe was mounted in place and the concentricity of the stylus with respect to the spindle axis was calibrated.
B. Data acquisition phase:

- The calibration sphere was measured by contacting the stylus of the touch-trigger probe at five different points on the calibration sphere.
- For rotation in the C-axis, 36 positions of the calibration sphere were considered, ranging from 0° to 360° with increments of 10°.
- Similarly, for the rotary A-axis, 13 positions of the calibration sphere were considered, ranging from -90° to +30° with increments of 10°.

C. Data arrangement and calculation phase:

- The data obtained for each position of the sphere was measured based on the five points located at positions Xc+, Xc-, Yc+, Yc-, and Zc- of the sphere, where the letter "c" represents the contact point between the probe and the calibration sphere while the variables X, Y, and Z represent the direction of contact. The sign "-" represents the up to down movement of the probe, for each one of the contact points with coordinates X, Y, and Z. This protocol was designed to calculate an accurate center for the calibration sphere at each of the 49 positions: 36 positions for the C-axis and 13 positions for the A-axis.
- The five-point set was arranged into four different combinations: {Xc+, Xc-, Yc+, Zc-}, {Xc+, Xc-, Yc-, Zc-}, {Xc+, Yc+, Yc-, Zc-}, and {Xc-, Yc+, Yc-, Zc-}, where each arrangement contained the Zc- point of the sphere. This avoids an error in the Z axis, which commonly occurs when the other four points are in the X-Y plane.
- After each set was obtained, the four obtained centers were combined and averaged, and the resultant value was taken as the center of that position. Thus, 36 centers for the C-axis and 13 centers for the A-axis can be calculated.

3 METHODS FOR CENTER CALCULATIONS

3.1 Calibration Sphere Center Calculation

The calculation was carried out based on a modified circle equation that solves for three coordinates instead of two, as expressed by Equation (3.1):

$$(X\text{-}Xc)^2 + (Y\text{-}Yc)^2 + (Z\text{-}Zc)^2 = r^2 \tag{3.1}$$

This equation can be used to calculate a sphere with an (Xc, Yc, Zc) center and radius r. However, to fit the needs of the calculation, it is necessary to re-formulate the equation as given in Equation (3.2):

$$X^2 + A_X + Y^2 + B_Y + Z^2 + C_Z + R_s = 0 \tag{3.2}$$

where X, Y, and Z represent the measured coordinate values, A_X, B_Y, and C_Z are the unknown variables to be calculated, and R_s is the variable for calculating the radius of the sphere. For example, Table 1 presents the data for the C-axis positions at 0°, 120°, and 240°, containing a set of five contact points each; these were subsequently separated into four combinations to calculate the values of the X, Y, Z coordinates of the center and the radius.

Position	C-axis F-10 mm/min.
0°	P1 = [353.523, -296.1, -110]
	P2 = [384.411, -296.1, -110]
	P3 = [369.7, -281.139, -110]
	P4 = [369.7, -312.004, -110]
	P5 = [369.7, -296.1, -95.636]
120°	P6 = [332.216, -445.201, -110]
	P7 = [358.607, -445.201, -110]
	P8 = [345.399, -430.102, -110]
	P9 = [345.399, -458.601, -110]
	P10 = [345.399, -445.201, -95.638]
	P11 = [216.005, -349.606, -110]
	P12 = [242.421, -349.606, -110]

240°	P13 = [228.424, -335.096, -110]
	P14 = [228.424, -365.026, -110]
	P15 = [228.424, -349.606, -95.629]

Table 1: Set-points protocol for C-axis at 0°, 120°, and 240°.

3.2 Rotary Axis Center Calculation

After the center of the calibration sphere for each position was calculated, the center of the rotary axes C and A had to be calculated. There are three center points in space that do not lie in the same plane as the machine's center coordinates. Therefore, the first step was to create a plane S in which all the three points lie in a plane that is not parallel to the machine's coordinate frame. This plane can be used to solve the system of a circle in a two-dimensional space. The easiest way to achieve this is to use the linear algebra equation expressed by Equation (3.3).

$$V = a \cdot V1 + b \cdot V2 \tag{3.3}$$

Any vector in this plane can be generated as a linear combination of the two non-parallel vectors, namely, V1 and V2, which are also called the base-vectors. The system of equations was then solved to determine the vectors perpendicular to V1 and V2 and to determine the center, which also corresponds to the center of the rotary axis (C-axis), as shown in Figure 2. Subsequently, a normal vector $\vec{N}$ perpendicular to the plane S can be calculated using the cross-product method of the two base vectors and moving it to the origin. In this case, the center of the circle that was already calculated can be better understood by examining Figure 2. This process was the same for both the A- and C-axis.

Since the circle calculations were carried out in the S plane, which is non-parallel to the coordinate frame of the machine, the normal vector $\vec{N}$ was also non-parallel to the machine's normal vector $\vec{Z}$. The angle (α) created by the tilted vector $\vec{N}$ and vector $\vec{Z}$ is therefore the angle deviation of the machine, which is normally very small. The angle was determined by Equation (3.4), as follows:

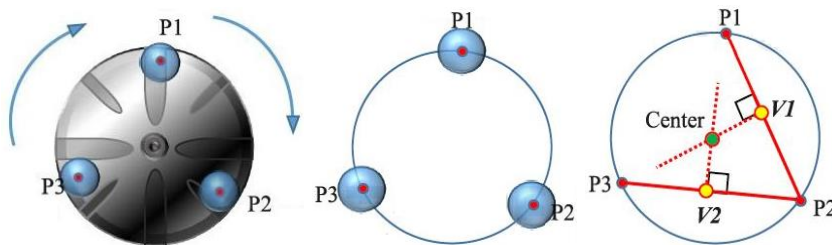$$cos(\alpha) = \frac{\vec{N} \bullet \vec{Z}}{|\vec{N}| \cdot |\vec{Z}|} \tag{3.4}$$

Figure 2: C-axis center calculation flow.

4 CALCULATION OF LOCATION ERRORS

Once centers and the normal vectors of rotary axes C and A are calculated, the data required to calculate the machine location errors can also be obtained. By ISO definition, these errors consist of the rotary axes position, rotary axes orientation, and zero position or offset. According to ISO 230-7, the machine errors for the rotary axis are as presented in Table 2. In this case, for the rotary axis C, XOC is the X position of C, YOC is the Y position of C, AOC is the squareness of C to Y, and BOC is the squareness of C to X, Figure 3 illustrates this relationship with more clarity. In Figure 3, the location errors of the C axis are illustrated more clearly, where XOC is the X value of

the coordinate where vector $\vec{N}$ crossed the plane XY, and YOC is the Y value of the coordinate where vector $\vec{N}$ crossed the plane XY. AOC is the angle between the projection of vector $\vec{N}$ in the YZ plane and the Z axis of the machine. The BOC error is the angle between the projection of vector $\vec{N}$ in the XZ plane and the Z axis of the machine, and the angle deviation is the angle between vector $\vec{N}$ and the Z axis of the machine.

C - axis	A - axis	B - axis
XOC	YOA	XOB
YOC	ZOA	ZOB
AOC	BOA	AOB
BOC	COA	COB

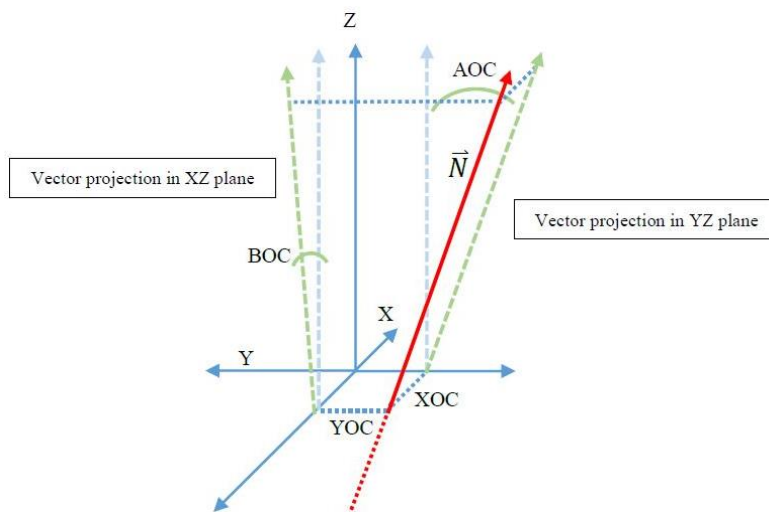**Table 2**: Location error nomenclature.

Figure 3: Location errors in C-axis.

Figure 4 illustrates the relationships among the calculated center, the normal vector, and the machine coordinate frame. The XOC and YOC errors can be calculated by Equation (4.1).

$$P_{xy} = Cxy - \left(\frac{Cxy(z)}{\vec{N}(z)} \right) \cdot \vec{N} \qquad (4.1)$$

where, P_{xy} is the intersection point between vector $\vec{N}$ and the XY plane, and Cxy is the center of the calculated circle. $Cxy(z)$ denotes the Z-component of the calculated center Cxy and $\vec{N}(z)$ denotes the Z-component of the vector $\vec{N}$. The X and Y coordinates of point P_{xy} correspond to the XOC and YOC values. In the same way, the errors of the titling axis were calculated after calculating the centers of each position of the sphere.
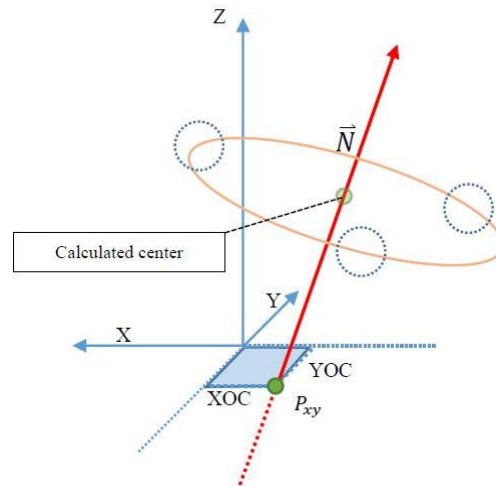
Figure 4: $\vec{N}$ vector and the center offset in C-axis.

5   PROGRAMMING STAGES TO OBTAIN LOCATION ERRORS

The computer program used to calculate the location errors can be divided into four different stages. Stage one consists of declaring the global variables and the input data. In this stage, the sphere position is also plotted by using the center of each sphere as a reference. This plotted diagram provides a better idea about the set of points by representing them graphically and aids during the debugging stage if there is a problem with the dataset prior to the calculation. The second stage consists of the rotary axis center calculations. As illustrated in Figure 2, three positional data points are required to calculate the center position and the normal vector for a rotary axis. Because 36 data points were measured on the C-axis and 13 data points were measured on the A-axis in this study, the number of combinations was 7,140 and 286 for the C-axis and A-axis, respectively. The operations in this stage necessitated iterations based on the different combinations calculated previously. The third stage consisted in calculating the errors of the AC-type CNC machine tool. The calculation for the A-axis was performed using the same procedure as that for the calculation for the C-axis but with a different reference to the nomenclature presented in Table 2 with regard to the description of each axis. The fourth stage consisted of the program managing the processing of the calculated data to obtain a more accurate result. This was achieved by eliminating a few of the calculated errors, as they may compromise the accuracy of the calculations. To illustrate an example of this, this paper here presents the result of calculating the YOC errors for a set of 7,140 points. To understand the behavior of the set of data points, this study utilized the tools included in MATLAB to plot and fit data to different types of distributions and to understand which distribution best represents the dataset. Figure 5 plots the data in terms of frequency.

In Figure 5, it can be easily seen that the distribution is not symmetrical, meaning that some points are too far away from each other. This clearly affects the way by which the mean and sigma of the bell are calculated. To demonstrate this, this study proceeded to calculate the normal distribution for the entire dataset and then superimposed the data onto the same figure in order compare how they fit in comparison to already plotted data. The result is depicted in Figure 6.
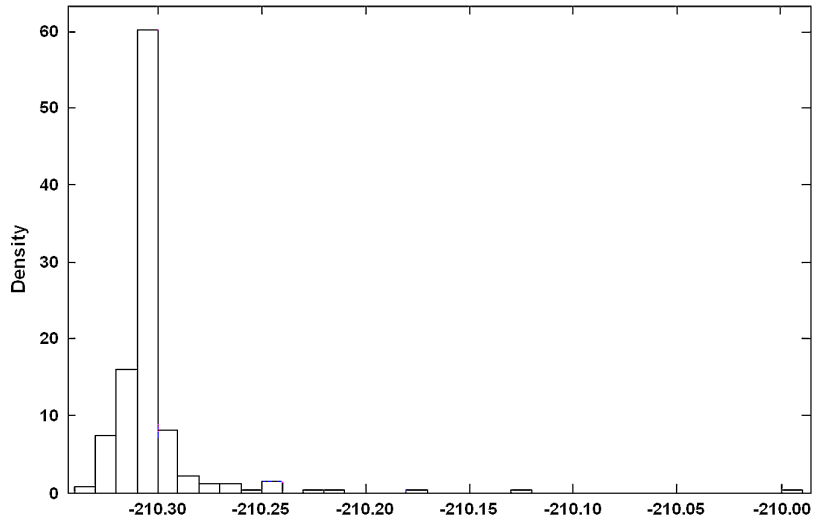
Figure 5: YOC value frequency plot. (Data on the horizontal axis denotes the calculated YOC error values.)
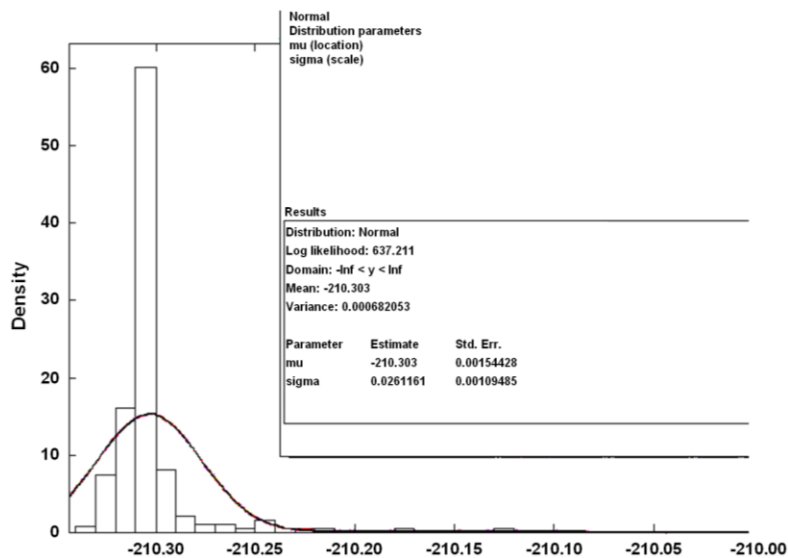

Figure 6: Normal distribution for entire dataset of YOC error. (Data on horizontal axis denotes the calculated YOC error values.)

The graph clearly shows that there are many points affecting the behavior of the system's normal distribution. In this case, the normal distribution does not represent data accurately since it has a significant number of outliers and is heavily populated in the vicinity of the mean. MATLAB contains other types of distributions that can be used to represent the data better. The t-location scale distribution is a robust distribution that can handle datasets similar to the one considered here. Applying the t-location scale distribution to the data, a better fit is obtained as illustrated in Figure 7.
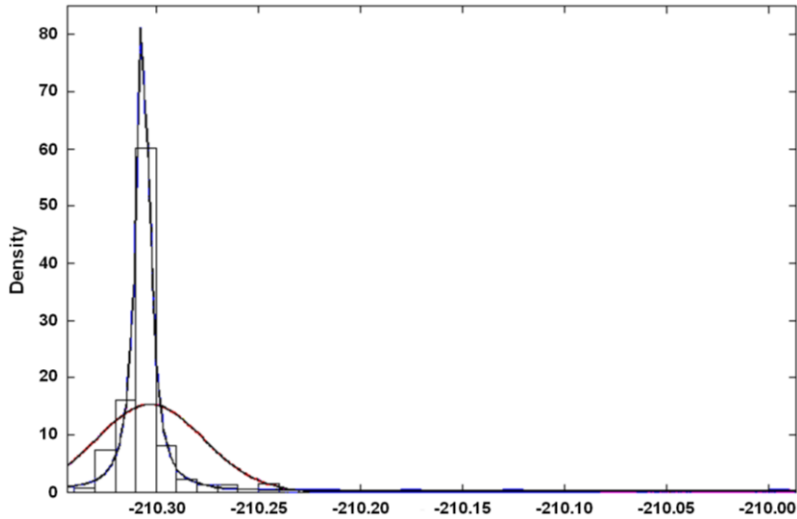
Figure 7: Entire dataset of YOC error with t-location scale distribution. (Data on horizontal axis denotes the calculated YOC error values.)

However, it was clear that the outlier points were caused by measurement failure. To prove this, the points that were too far away from the mean were excluded in this study and the normal distribution was re-applied. Figure 8 illustrates the test results after various points were excluded.
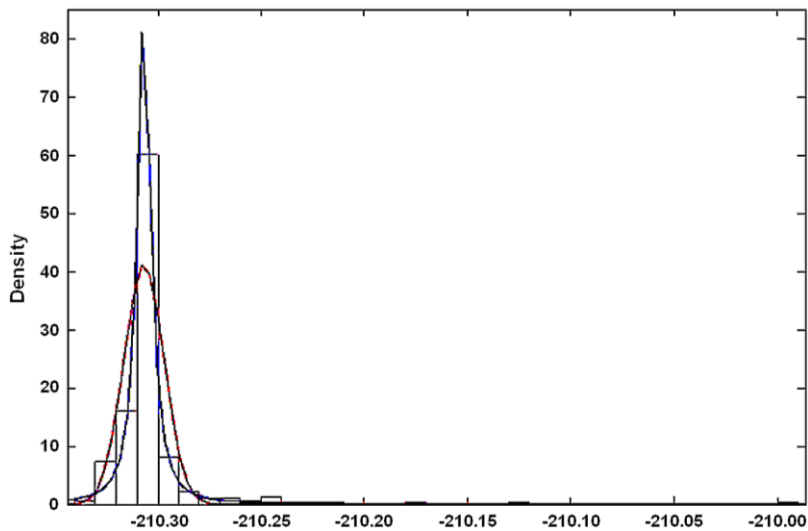

Figure 8: Normal distribution after excluding YOC. (Data on horizontal axis denotes the calculated YOC error values.)

An obvious improvement was observed in the results but it was noticed that it could be improved further to obtain the most possible set of accurate points. After analyzing the obtained data values, it was observed that there existed many points that were far away from the mean. However, there also existed a lot of points in the vicinity of the mean that could also compromise the accuracy of the calculation. These erroneous results were caused due to a number of center position

combinations that are unsuitable for error measurement. This happens when the chosen points are too close to each other. The closer the points are to each other, the higher is the tendency of the calculated circle to turn into a line, and the center value to move towards infinity, as depicted in Figure 9.
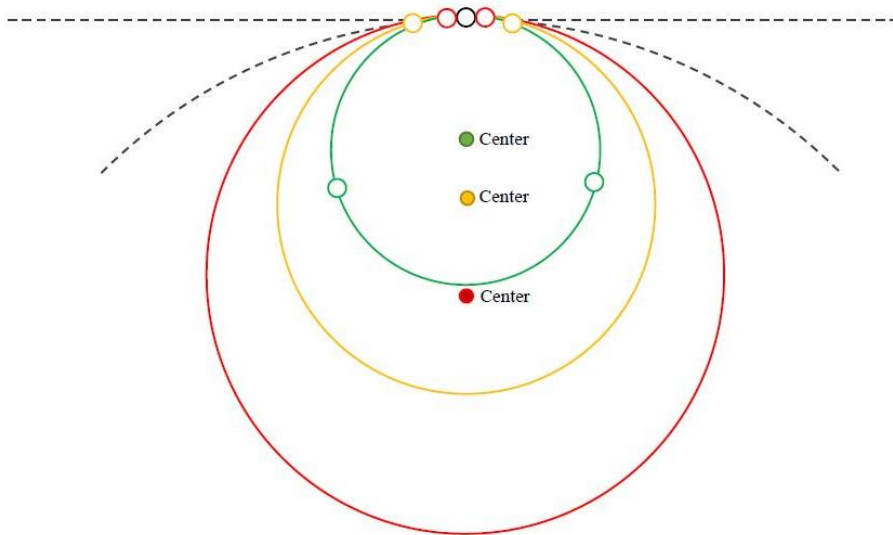

Figure 9: Failed calculations due to proximity between points.

To solve this problem, an algorithm to divide the filtering procedure into two stages was implemented in the beginning of the combination selection process for the C-axis. The algorithm restricted the combinations to a set of points in which the positions between each point summed to a total of 360° with a difference of at least 30° between them in order to ensure that the chosen points had a specific distribution around the real center. As an example, consider the following set of points: a = 0°, b = 30°, and c = 80°. This set has a total of 360° and the difference between the points is 30° between a–b, 50° between b–c, and 280° between c-a. The case of the A-axis is slightly different since the tilting axis did not carry out a full revolution and this study considered that the negative maximum and positive maximum positions as the limits. For this dataset, the negative maximum was -90° and the positive maximum was 30°; moreover, the difference between adjacent positions must be at least 30°. As an example, consider the dataset a = -80°, b = 0°, and c = 30°. For this set, the difference between the positions was 80° between a–b and 30° between b–c. Since the axis did not carry out a full revolution, the c-a distance was not considered.

After this method was applied and the combinations were calculated, the elements contained in the set of points were less but had higher accuracy. Before applying the pre-filtering stage, this study contained a set of points with 7,140 combinations for the C-axis and 286 combinations for the A-axis. After the method was implemented to remove the combinations that caused the calculation results to significantly deviate from the mean value and to remove the combinations in which the chosen data points were too close to each other, the 7,140 combinations were reduced to only 2,925 points, which represented 40.96% of the original set. Additionally, the 286 combinations for the A-axis set were reduced to only 13, which accounted for 4.54% of the set. The improvement in data quality can be seen in Figure 10. It can be seen that the resulting data is more similar to the shape desired for a normally distributed set of points, which means that the proposed approaches successfully removed the points that were not meaningful to the calculations.

The reduction of data size also reduced the computation time to almost two thirds in comparison to the original time.
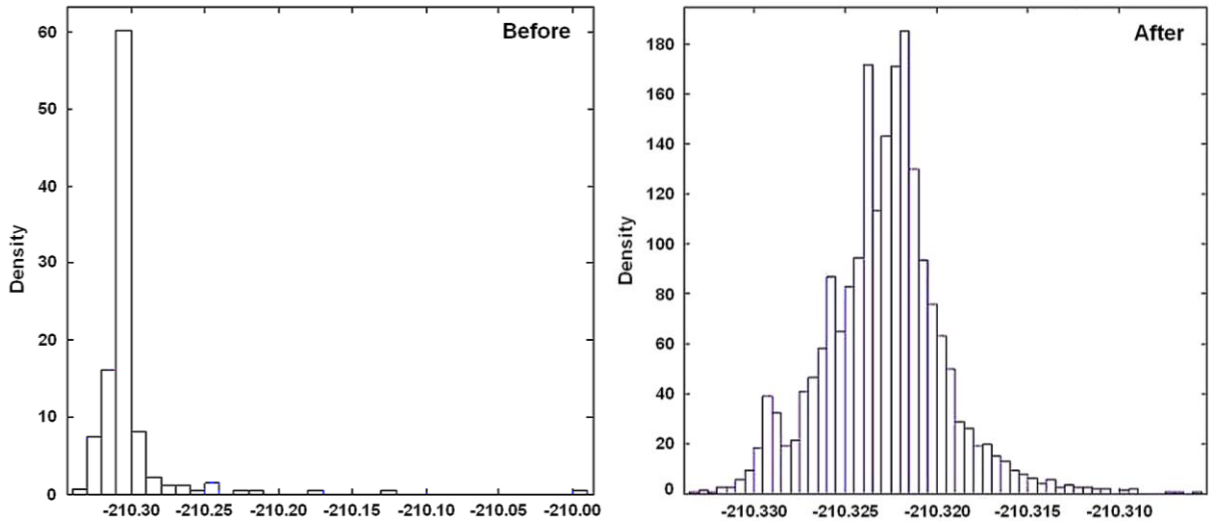

Figure 10: Before and after data pre-filtering stage.

The second stage of filtering was executed once the errors were calculated and stored in an array. In this stage this study used two equations: Equation (5.1) to calculate the mean of the data represented by μ, and Equation (5.2) to calculate the σ value representing the variance of the calculation. After both equations were implemented, Equation (5.3) was used to eliminate the tails of the bell.

$$\mu = \frac{\sum_{t=1}^{N} X_i}{N} = \frac{\sum X}{N} \tag{5.1}$$

$$\sigma^2 = \frac{\sum (X - \mu)^2}{N} \tag{5.2}$$

$$\tau = \mu \pm \frac{\sigma}{2} \tag{5.3}$$

τ indicates the threshold for data. Once Equation (5.3) was applied, μ and σ were calculated once more, but this time the μ value represented final result, while σ represented the calculation error variance. Thus, it was able to calculate the error and sigma for each calculation of the location error and this made it manageable to update the machine controller. The results calculated after the filtering process are presented in Table 3.

Definition	Values from the machine	Values from the calculation	Difference
XOC	-350.7675	-350.7881	-0.0206
YOA	-210.3166	-210.3227	-0.0061
ZOA	-549.3474	-549.3371	0.0103
T-Offset Y	-0.0167	-0.0174	0.0508
T-Offset Z	0.0925	0.1118	0.0193
YOC	-	-210.3152	-
AOC	-	0.00001	-

BOC	-	0.00000	-
COA	-	0.00000	-
BOA	-	0.00001	-
Angle deviation C	-	0.00001	-
Angle deviation A	-	0.00001	-

Table 3: Location error calculation using two-stage filtering approach.

The values from the machine were set by the machining tool manufacturer using a commercial measurement software that utilizes the conventional least squares method to calculate location errors, as shown in Table 3. A real cutting test was carried out using the data calculated by the commercial software and the data obtained by the program developed in this study to verify the calculation results presented in this study.

6   VALIDATION OF THE DEVELOPED METHODS

There are many ways to calculate the errors present in machining centers. However, the measurement devices and systems produced by various companies in order to carry out such calculations are prone to error. Even though these methods, developed by many different companies, claim to be reliable, well-known, and capable of obtaining the best results in the market, from a research point of view, it is difficult to say which one is the most accurate and provides the best direction to follow. To validate the developed method and ensure that it is at least comparable to already existing approaches, a real test had to be carried out. Such a test was developed by a machining tool company, and consists of cutting the surface of a square shaped workpiece into nine different sections. Accordingly, it is called the nine sections test. In this test, each section is machined by using a combination of angles for the rotary axes of the five-axis CNC machine tool. The first section was cut in the center at A = 0 and C = 0. Then, this section was taken as the reference, and the rest of the sections were measured and compared to the first section by using a micrometer. The accuracy of the machine is considered to be better when the height of the sections is closer to each other.

The experiment was executed on an aluminum workpiece using a round-tip milling tool. The test was carried out with a spindle speed of 6,000 rpm and feed rate 600 mm/min. The test results indicate the depth variation of each section in comparison to the center. Therefore, the test results obtained positive or negative values depending on the machining error. Figure 11 illustrates how the workpiece was divided, the sequence of the machined sections, and the angles used in each section. First, the test was conducted by using the parameters calculated by the commercialized measurement software. Then, the piece was measured, and the same setup was used in the second test, but with the values updated based on the calculation results of this study presented in Table 3. Figure 12 shows the results of the last test using the calculated parameters. To make the results more comprehensible, the final result of both tests is represented in Figure 13. Table 4 presents the numerical and statistical results for the different tests. Here, all measurements and compensation processes were performed under similar temperature (around 28°C) and air humidity (relative humidity around 75%) for a fair comparison. For the test conducted with the values from the machine, the maximum value of the errors was -15 μm and occurred at sections 5, 8, and 9. The average value of errors (AVG), maximum value of absolute errors (MAX), and root-mean-square value of errors (RMS) were -9.8889 μm, 15 μm, and 10.9697 μm, respectively. The test results revealed that the height errors were quite large and varied significantly. Therefore, the values from the machine could not exactly compensate for the location errors of the five-axis CNC machine tool. On the other hand, the height errors were significantly reduced by applying the values obtained from the calculation proposed in this study. The maximum value of the errors was -3 μm and occurred at section 8 where the A-axis was located at -30° and the C-axis was located at 270°. The AVG value was -0.1111 μm and was much smaller than that of the first test. A

98.88% rate of improvement was achieved. The RMS value was 1.7321 µm which was also much smaller than that of the first test. An 84.21% rate of improvement was achieved. This clearly demonstrated the preciseness of the calculation of location errors and the feasibility of the programming process proposed in this study.
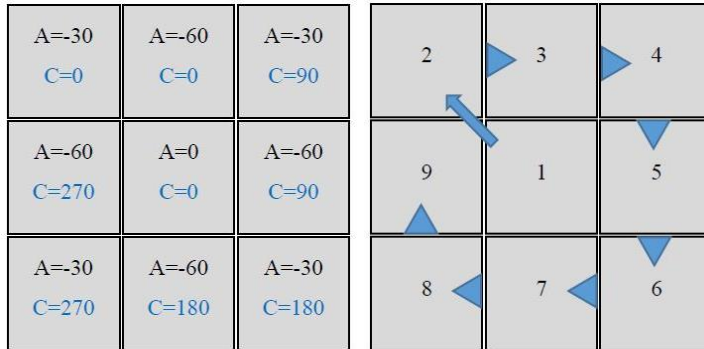
A=-30 C=0	A=-60 C=0	A=-30 C=90
A=-60 C=270	A=0 C=0	A=-60 C=90
A=-30 C=270	A=-60 C=180	A=-30 C=180

2	3	4
9	1	5
8	7	6

Figure 11: Rotary axes parameters and machining path.
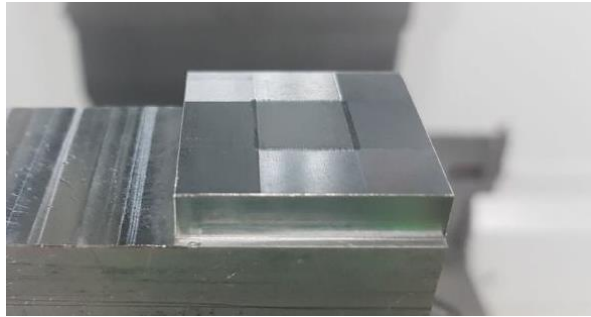
Figure 12: Workpiece after cutting test.

Using first test values		
-5	-9	-11
-15	0	-15
-15	-10	-9

Using calculated values		
+2	+2	+2
0	0	-1
-3	-1	-2
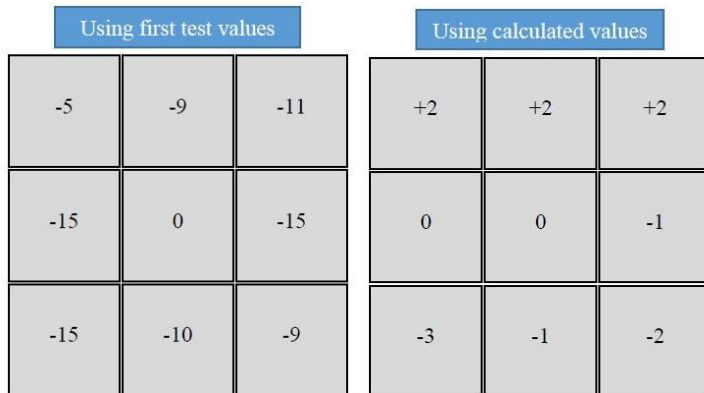
Figure 13: First and second test results.

Section	1	2	3
Values from the machine (µm)	0	-5	-9

Section	4	5	6
Values from the machine (μm)	-11	-15	-9
Section	7	8	9
Values from the machine (μm)	-10	-15	-15
AVG	-9.8889		
MAX	15		
RMS	10.9697		
Section	1	2	3
Values from the calculation (μm)	0	2	2
Section	4	5	6
Values from the calculation (μm)	2	-1	-2
Section	7	8	9
Values from the calculation (μm)	-1	-3	0
AVG (rate of improvement)	-0.1111 (98.88%)		
MAX (rate of improvement)	3 (80.00%)		
RMS (rate of improvement)	1.7321 (84.21%)		

Table 4: Numerical results for different tests of nine sections.

7   CONCLUSIONS

In this paper, a method for calculating location errors particular to five-axis CNC machine tools using touch-trigger probe and calibration sphere was presented. The five-axis CNC machine tool generally has 43 errors (including component errors and location errors) that significantly depend on the manufacturing and assembly processes of the machine tool. The significant error source of the touch-trigger probe primarily depends on the speed of the touch-trigger probe before contacting the standard calibration sphere. The proposed method, that consists of different steps in the selection, arrangement, calculation, and final filtering of the data, was able to obtain an accurate result with a precision restricted only by the resolution of the dataset. The standard calibration sphere center calculation method was also tested and verified. The calculation with regard to the axes was based on ISO standards and the calculation procedure was verified using different point sets with different data sizes and possible combinations to establish the stability and reliability of the calculation. A computer program was also developed for handling the calculations pertaining to five-axis CNC machine tools with an AC-type configuration. The filtering stage of the process was shown to drastically improve the results obtained by the calculation and provided a reliable output of meaningful data while excluding points that could have compromised the results. To validate the performed calculations a real test was carried out, and it provided significantly better results by successfully achieving the objectives described in this paper.

It can be concluded from this study that high accuracy and well-calibrated instruments should be used and that more time should be dedicated to the environment setup stage, since the reliability of the data depends on the accuracy of the acquired data. Moreover, choosing a good set of points ensures accuracy when calculating machine errors. Furthermore, the instruments should be managed carefully and any manipulation that may compromise their accuracy should be avoided. The statistical characteristics of the measurement data and all the possible combinations must be further considered for reducing the effects of variation on the calculation results. This study focused on the design of the calculation and programming processes to significantly improve the calculation results for the measurement of the geometric errors of a five-axis CNC machine tool using acquired data points that could be contaminated during the touch-trigger probe

measurement processes. This study considered the statistical characteristics of the measured data points and their possible combinations to reduce the effects of measurement errors on the calculation results. The cutting test, which is generally used by manufacturers to evaluate the motion performances of a five-axis CNC machine tool, successfully validated the approach developed in this study.

ACKNOWLEDGEMENTS

REFERENCES

[1] Alessandro, V.; Gianni, C.; Antonio, S.: Axis Geometrical Errors Analysis through a Performance Test to Evaluate Kinematic Error in a Five Axis Tilting-Rotary Table Machine Tool, Precision Engineering, 39, 2015, 224-233. http://doi.org/10.1016/j.precisioneng.2014.09.007

[2] Bi, Q.; Huang, N.; Sun, C.; Wang, Y.; Zhu, L.; Ding, H.: Identification and Compensation of Geometric Errors of Rotary Axes on Five-Axis Machine by on-Machine Measurement, International Journal of Machine Tools and Manufacture, 89, 2015, 182-191. http://doi.org/10.1016/j.ijmachtools.2014.11.008

[3] Bohan, Z.; Feng, G.; Yan, L.: Study on Pre-Travel Behaviour of Touch Trigger Probe under Actual Measuring Conditions, Proc. 13th CIRP Conference on Computer Aided Tolerancing, CAT 2014, 2015, 53-58. http://doi.org/10.1016/j.procir.2015.04.043

[4] Chen, Y.; Zhao, X.; Gao, W.; Hu, G.; Zhang, S.; Zhang, D.: A Novel Multi-Probe Method for Separating Spindle Radial Error from Artifact Roundness Error, International Journal of Advanced Manufacturing Technology, 2017, 1-12. http://doi.org/10.1007/s00170-017-0533-5

[5] Estler, T. W.; Phillips, S. D.; Borchardt, B.; Hopp, T.; Witzgall, C.; Levenson, M.; Eberhardt, K.; McClain, M.; Shen, Y.; Zhang, X.: Error Compensation for CMM Touch Trigger Probes, Precision Engineering, 19(2-3), 1996, 85-97.

[6] Flynn, J. M.; Shokrani, A.; Vichare, P.; Dhokia, V.; Newman, S. T.: A New Methodology for Identifying Location Errors in 5-Axis Machine Tools Using a Single Ballbar Set-Up, International Journal of Advanced Manufacturing Technology, 2016, 1-19. http://doi.org/10.1007/s00170-016-9090-6

[7] Gebhardt, M.; Mayr, J.; Furrer, N.; Widmer, T.; Weikert, S.; Knapp, W.: High Precision Grey-Box Model for Compensation of Thermal Errors on Five-Axis Machines, CIRP Annals - Manufacturing Technology, 63(1), 2014, 509-512. http://doi.org/10.1016/j.cirp.2014.03.029

[8] Hong, C.; Ibaraki, S.; Matsubara, A.: Influence of Position-Dependent Geometric Errors of Rotary Axes on a Machining Test of Cone Frustum by Five-Axis Machine Tools, Precision Engineering, 35(1), 2011, 1-11. http://doi.org/10.1016/j.precisioneng.2010.09.004

[9] Hsu, Y. Y.; Chang, C. H.; Tsai, Y. T.: Modeling and Identification for Rotary Geometric Errors of Five-Axis Machine Tools with R-Test Measurement, Proc. ASME 2012 International Design Engineering Technical Conferences and Computers and Information in Engineering Conference, IDETC/CIE 2012, Chicago, IL, 2012, 567-575. http://doi.org/10.1115/DETC2012-70182

[10] Huang, N.; Zhang, S.; Bi, Q.; Wang, Y.: Identification of Geometric Errors of Rotary Axes on 5-Axis Machine Tools by on-Machine Measurement, International Journal of Advanced Manufacturing Technology, 84(1-4), 2016, 505-512. http://doi.org/10.1007/s00170-015-7713-y

[11] Ibaraki, S.; Iritani, T.; Matsushita, T.: Calibration of Location Errors of Rotary Axes on Five-Axis Machine Tools by on-the-Machine Measurement Using a Touch-Trigger Probe, International Journal of Machine Tools and Manufacture, 58, 2012, 44-53. http://doi.org/10.1016/j.ijmachtools.2012.03.002

[12] Ibaraki, S.; Iritani, T.; Matsushita, T.: Error Map Construction for Rotary Axes on Five-Axis Machine Tools by on-the-Machine Measurement Using a Touch-Trigger Probe, International Journal of Machine Tools and Manufacture, 68, 2013, 21-29. http://doi.org/10.1016/j.ijmachtools.2013.01.001

[13] Ibaraki, S.; Kakino, Y.; Akai, T.; Takayama, N.; Yamaji, I.; Ogawa, K.: Identification of Motion Error Sources on Five-Axis Machine Tools by Ball-Bar Measurements (1st Report) - Classification of Motion Error Components and Development of the Modified Ball Bar Device (DBB5), Seimitsu Kogaku Kaishi/Journal of the Japan Society for Precision Engineering, 76(3), 2010, 333-337. http://doi.org/10.2493/jjspe.76.333

[14] Ibaraki, S.; Nagai, Y.; Otsubo, H.; Sakai, Y.; Morimoto, S.; Miyazaki, Y.: R-Test Analysis Software for Error Calibration of Five-Axis Machine Tools: Application to a Five-Axis Machine Tool with Two Rotary Axes on the Tool Side, International Journal of Automation Technology, 9(4), 2015, 387-395.

[15] Ibaraki, S.; Ota, Y.: Error Calibration for Five-Axis Machine Tools by on-the-Machine Measurement Using a Touch-Trigger Probe, International Journal of Automation Technology, 8(1), 2013, 20-27.

[16] Ibaraki, S.; Ota, Y.: A Machining Test to Calibrate Rotary Axis Error Motions of Five-Axis Machine Tools and Its Application to Thermal Deformation Test, International Journal of Machine Tools and Manufacture, 86, 2014, 81-88. http://doi.org/10.1016/j.ijmachtools.2014.07.005

[17] Ibaraki, S.; Oyama, C.; Otsubo, H.: Construction of an Error Map of Rotary Axes on a Five-Axis Machining Center by Static R-Test, International Journal of Machine Tools and Manufacture, 51(3), 2011, 190-200. http://doi.org/10.1016/j.ijmachtools.2010.11.011

[18] Ihara, Y.; Nagasawa, T.: Fundamental Study of the on-Machine Measurement in the Machining Center with a Touch Trigger Probe, International Journal of Automation Technology, 7(5), 2013, 523-536.

[19] Jankowski, M.; Wozniak, A.: Mechanical Model of Errors of Probes for Numerical Controlled Machine Tools, Measurement: Journal of the International Measurement Confederation, 77, 2016, 317-326. http://doi.org/10.1016/j.measurement.2015.09.023

[20] Jankowski, M.; Woźniak, A.: Master Artifacts for Testing the Performance of Probes for CNC Machine Tools, Proc. Advances in Intelligent Systems and Computing, 2016, 323-328. http://doi.org/10.1007/978-3-319-23923-1_49

[21] Jiang, Z.; Bao, S.; Zhou, X.; Tang, X.; Zheng, S.: Identification of Location Errors by a Touch-Trigger Probe on Five-Axis Machine Tools with a Tilting Head, International Journal of Advanced Manufacturing Technology, 81(1-4), 2015, 149-158. http://doi.org/10.1007/s00170-015-7189-9

[22] Jiang, Z.; Song, B.; Zhou, X.; Tang, X.; Zheng, S.: On-Machine Measurement of Location Errors on Five-Axis Machine Tools by Machining Tests and a Laser Displacement Sensor, International Journal of Machine Tools and Manufacture, 95, 2015, 1-12. http://doi.org/10.1016/j.ijmachtools.2015.05.004

[23] Jiang, Z.; Tang, X.; Zhou, X.; Zheng, S.: Machining Tests for Identification of Location Errors on Five-Axis Machine Tools with a Tilting Head, International Journal of Advanced Manufacturing Technology, 79(1-4), 2015, 245-254. http://doi.org/10.1007/s00170-015-6838-3

[24] Kiridena, V.; Ferreira, P. M.: Mapping the Effects of Positioning Errors on the Volumetric Accuracy of Five-Axis CNC Machine Tools, International Journal of Machine Tools and Manufacture, 33(3), 1993, 417-437. http://doi.org/10.1016/0890-6955(93)90049-Z

[25] Lasemi, A.; Xue, D.; Gu, P.: Accurate Identification and Compensation of Geometric Errors of 5-Axis CNC Machine Tools Using Double Ball Bar, Measurement Science and Technology, 27(5), 2016. http://doi.org/10.1088/0957-0233/27/5/055004

[26] Lei, W. T.; Wang, W. C.; Fang, T. C.: Ballbar Dynamic Tests for Rotary Axes of Five-Axis CNC Machine Tools, International Journal of Machine Tools and Manufacture, 82-83, 2014, 29-41. http://doi.org/10.1016/j.ijmachtools.2014.03.008

[27] Li, R. J.; Xiang, M.; He, Y. X.; Fan, K. C.; Cheng, Z. Y.; Huang, Q. X.; Zhou, B.: Development of a High-Precision Touch-Trigger Probe Using a Single Sensor, Applied Sciences (Switzerland), 6(3), 2016. http://doi.org/10.3390/app6030086

[28] Mayer, J. R. R.: Five-Axis Machine Tool Calibration by Probing a Scale Enriched Reconfigurable Uncalibrated Master Balls Artefact, CIRP Annals - Manufacturing Technology, 61(1), 2012, 515-518. http://doi.org/10.1016/j.cirp.2012.03.022

[29] McHichi, N. A.; Mayer, J. R. R.: Axis Location Errors and Error Motions Calibration for a Five-Axis Machine Tool Using the SAMBA Method, Procedia CIRP, 14, 2014, 305-310. http://doi.org/10.1016/j.procir.2014.03.088

[30] Nagai, Y.; Ibaraki, S.; Nishikawa, S.: Error Calibration of Five-Axis Machine Tools by on-Machine Measurement System Using a Laser Displacement Sensor, Journal of Advanced Mechanical Design, Systems and Manufacturing, 8(4), 2014, http://doi.org/10.1299/jamdsm.2014jamdsm0053

[31] Qian, X.; Zhao, P.; Lou, P.: An on-Machine Measurement Method for Touch-Trigger Probe Based on RBFNN, Research Journal of Applied Sciences, Engineering and Technology, 5(3), 2013, 909-913.

[32] Rahman, M. M.; Mayer, R.: Calibration Performance Investigation of an Uncalibrated Indigenous Artefact Probing for Five-Axis Machine Tool, Journal of Machine Engineering, 16(1), 2016, 33-42.

[33] Wozniak, A.; Byszewski, M.; Jankowski, M.: Setup for Triggering Force Testing of Touch Probes for CNC Machine Tools and CMMs, Measurement Science Review, 13(1), 2013, 29-33. http://doi.org/10.2478/msr-2013-0004

[34] Wozniak, A.; Jankowski, M.: Wireless Communication Influence on CNC Machine Tool Probe Metrological Parameters, International Journal of Advanced Manufacturing Technology, 82(1-4), 2016, 535-542. http://doi.org/10.1007/s00170-015-7374-x

[35] Wozniak, A.; Jankowski, M.: Variable Speed Compensation Method of Errors of Probes for CNC Machine Tools, Precision Engineering, 49, 2017, 316-321. http://doi.org/10.1016/j.precisioneng.2017.03.001

[36] Xiang, S.; Altintas, Y.: Modeling and Compensation of Volumetric Errors for Five-Axis Machine Tools, International Journal of Machine Tools and Manufacture, 101, 2016, 65-78. http://doi.org/10.1016/j.ijmachtools.2015.11.006

[37] Xue, K.; Kurella, V.; Spence, A.: Multi-Sensor Blue LED and Touch Probe Inspection System, Computer-Aided Design and Applications, 13(6), 2016, 827-834. http://doi.org/10.1080/16864360.2016.1168226

[38] Zhang, R.; Wang, Y. P.: On-Machine Measurement System Implemented Based on Fanuc CNC System Using a Touch Trigger Probe, Proc. 5th International Conference on Mechanical and Aerospace Engineering, ICMAE 2014, Madrid, 2014, 3-7. http://doi.org/10.4028/www.scientific.net/AMR.1016.3

[39] Zhang, Z.; Hu, H.: A General Strategy for Geometric Error Identification of Multi-Axis Machine Tools Based on Point Measurement, International Journal of Advanced Manufacturing Technology, 69(5-8), 2013, 1483-1497. http://doi.org/10.1007/s00170-013-5094-7